Microwave Detection of Electron-Phonon Interactions in a Cavity-Coupled Double Quantum Dot

T. R. Hartke, Y.-Y. Liu, M. J. Gullans, and J. R. Petta

Department of Physics, Princeton University, Princeton, New Jersey 08544, USA

Quantum confinement leads to the formation of discrete electronic states in quantum dots. Here we probe electron-phonon interactions in a suspended InAs nanowire double quantum dot (DQD) that is electric-dipole coupled to a microwave cavity. We apply a finite bias across the wire to drive a steady state population in the DQD excited state, enabling a direct measurement of the electron-phonon coupling strength at the DQD transition energy. The amplitude and phase response of the cavity field exhibit oscillations that are periodic in the DQD energy level detuning due to the phonon modes of the nanowire. The observed cavity phase shift is consistent with theory that predicts a renormalization of the cavity center frequency by coupling to phonons.

Phonons, the quantized lattice vibrations in a crystalline solid, are ubiquitous in condensed matter systems and impact the properties of bulk and nanostructured materials. For example, Raman scattering measurements provide a detailed probe of the phonon density of states in carbon nanotubes [1], and it is now known that phonons limit the maximum current in single nanotube devices [2–4]. Similarly, spin relaxation in semiconductors is generally governed by processes that involve phonon emission [5–7]. Electronic relaxation processes involving phonons can even be harnessed to cool mechanical degrees of freedom in nanostructures [8,9].

Semiconductor double quantum dots (DQDs) are well-suited for probing electron-phonon coupling [10–14] since inelastic interdot tunneling generally involves the spontaneous emission of a phonon in order to conserve energy [15]. Moreover, the DQD energy level difference is electrically tunable, which allows the effective electron-phonon coupling strength to be probed as a function of phonon energy. Confinement can further influence phonon modes in nanostructures, and new methods of controlled nanowire placement [16,17] may allow for careful engineering of the phonon spectrum in semiconductors, similar to recent optomechanics experiments with suspended carbon nanotubes [18–20].

In this Letter, we investigate the interplay of electrons, phonons, and photons in a cavity-coupled InAs nanowire DQD which is mechanically suspended in vacuum. The interaction of photons and electrons in DQDs has been studied extensively in the circuit QED architecture, where the charge dipole of a DQD is coupled to a microwave cavity [21–23]. A phonon sideband has recently been observed in DQD masers that are driven by single electron tunneling [24], and a related theory suggests that the detailed energy-dependence of the one-dimensional

nanowire phonon spectral density should have observable consequences in the photon emission rate [25], although this has not yet been observed. Here we measure the dc current I as a function of DQD energy level detuning ϵ and show that it exhibits periodic oscillations that are consistent with the phonon spectral density in a confined nanostructure [13,14]. Measurements of the cavity amplitude and phase response reveal the detailed energy dependence of the electron-phonon coupling and exhibit a response that is periodic in ϵ. We employ a microscopic theoretical model of the device that suggests that the dispersive cavity phase shift is due to a renormalization of the cavity center frequency by coupling to phonons [26].

The suspended nanowire DQD device is shown schematically in Fig. 1(a). A 50 nm diameter InAs nanowire [27,28] is manually placed across two lithographically defined Ti/Au pedestals using a long working distance optical microscope [16]. The pedestal thickness results in a 15 nm vacuum gap between the nanowire and Ti/Au electrostatic back gates (green) (V_{LW}, V_L, V_M, V_R, V_{RW}), which are used to produce the double-well confinement potential. In contrast to earlier experiments [23,29], the back gates are not coated with SiN_x dielectric. Instead, electrical isolation is achieved using the vacuum gap, which further confirms that the nanowire is physically suspended above the back gates. Ti/Au source (S) and drain (Cavity + D) contacts (red), with a separation of 380 nm, are deposited on top of the pedestals. A scanning electron microscope (SEM) image of a representative device is shown in Fig. 1(b).

In order to study the interaction of electrons in the DQD with photons in the cavity and phonons in the nanowire, the DQD is electric-dipole coupled to the voltage antinode of a Nb superconducting transmission line resonator (Cavity+ D) with resonance frequency $f_c = 7782.8$ MHz and quality
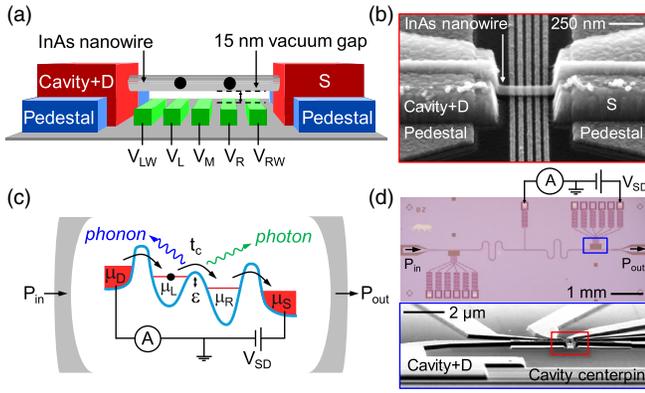
FIG. 1. (a) Schematic representation of the suspended InAs nanowire DQD. (b) Tilted angle SEM image of the device. (c) Energy level configuration of the DQD, which is placed inside a microwave cavity and probed by a weak microwave field. (d) Optical image of the microwave cavity in (c) (upper panel), and tilted angle SEM image showing the electrical connection between the drain contact of the DQD and the cavity centerpin (lower panel). The red box indicates the region shown in (b).

factor $Q \sim 3050$ [24,30]. A schematic diagram illustrating the key elements of the device is shown in Fig. 1(c). The electrical connection between the DQD and cavity is shown in Fig. 1(d). Electron-phonon coupling is probed by measuring the dc current through the DQD and the cavity amplitude and phase response as a function of ϵ [31]. Measurements are performed in a dilution refrigerator with a base temperature $T = 10$ mK.

Figure 2(a) shows the current I through the device as a function of the gate voltages V_L and V_R for $V_{SD} = 2.5$ mV. Nonzero current is observed within finite bias triangles, where the chemical potentials $\mu_D > \mu_L > \mu_R > \mu_S$. DQD charge states are labeled by (N_L, N_R), where N_L (N_R) is the number of electrons in the left (right) dot. We are able to reduce the electron number until no further charge transitions are observed (see the Supplemental Material [32]), although the data presented in this Letter are taken with $N_L \approx N_R \approx$ 4–6 to increase the current through the device and therefore the number of photon emission events [33,34].

Early experiments on semiconductor DQDs showed that energy is conserved during inelastic interdot tunneling through the spontaneous emission of a phonon [15]. Measurements of the current as a function of level detuning, $I(\epsilon)$, probe the environment at an energy $\Omega(\epsilon) = \sqrt{\epsilon^2 + 4t_c^2}$, where t_c is the interdot tunnel coupling. Oscillations in $I(\epsilon)$ were attributed to electron phonon coupling [13–15]. In contrast with these previous experiments, our DQD is electric-dipole coupled to a cavity. Therefore, energy can be emitted during interdot tunneling by processes that involve the emission of both a phonon and a photon [33], as illustrated in Fig. 1(c). Because of these higher-order emission processes, we may expect to see signatures of electron-phonon coupling in the amplitude and phase response of the cavity.

We first measure the current through the DQD and search for oscillations in $I(\epsilon)$ that are indicative of transitions between discrete electronic states that are accompanied by the emission of a phonon with energy $\Omega(\epsilon)$. To increase the visibility of the current oscillations at this particular charge transition we plot $\partial^2 I/(\partial V_L \partial V_R)$ as a function of V_L and V_R in Fig. 2(b) over the same gate voltage range as Fig. 2(a). These data reveal oscillations that are present throughout the inelastic region ($\epsilon \gg 0$) of the finite bias triangle. The oscillations are parallel to the interdot charge transition axis ($\epsilon = 0$) and therefore occur at a constant detuning, as expected for a decay mechanism that primarily depends on $\Omega(\epsilon)$. Figure 2(c) shows that small oscillations are directly visible in $I(\epsilon)$. A plot of $dI/d\epsilon$ (inset) shows that this current modulation has a periodic spacing of approximately 60 μeV which is consistent with expectations for the energy scale of phonons in the suspended nanowire device (see the Supplemental Material [32]) and larger than the energy scale of cavity photons ($hf_c \approx 32$ μeV). Current oscillations with a period of 60 ± 5 μeV were observed at more than 10 other charge transitions in the device, at forward and reverse bias [32].
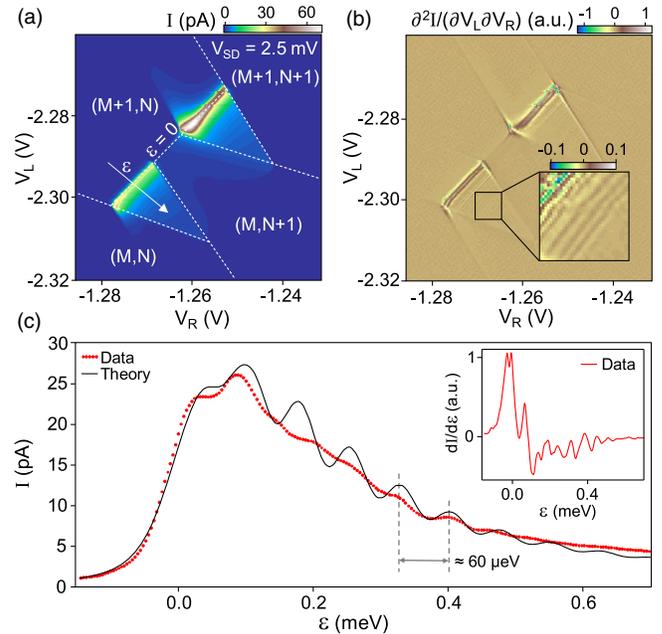

FIG. 2. (a) Current I through the DQD as a function of V_L and V_R with $V_{SD} = 2.5$ mV. The interdot level detuning ϵ is adjusted along the white arrow. (b) Second derivative $\partial^2 I/(\partial V_L \partial V_R)$ of the data in (a) show periodic oscillations as a function of ϵ. (c) I as a function of ϵ (red) accompanied by a simple theory prediction (black) that accounts for phonon emission. In the theory curve, we use the parameters: $t_c = 22$ μeV, $J(2t_c/\hbar)/2\pi = 0.3$ GHz, $d = 120$ nm, $\omega_0/2\pi = 130$ GHz, $c_n = 2100$ m/s, $r = 4 \times 10^{-3}$, $\Gamma_L/2\pi = \Gamma_R/2\pi = 90$ MHz and a nanowire temperature of 200 mK. Inset: $dI/d\epsilon$ as a function of ϵ showing oscillations with approximately 60 μeV periodicity in ϵ.

To better understand the observed oscillations in the current, we model the interaction of the DQD with the lattice phonons using a spin-boson model [10,11,13]

$$H = \frac{\Omega(\epsilon)}{2}\sigma_z + \sum_k \hbar\omega_k a_k^\dagger a_k + \hbar\sum_k \lambda_k \sigma_x(a_k + a_k^\dagger), \quad (1)$$

where σ_z is the Pauli matrix acting on the two charge states of the DQD, ω_k is the dispersion of a phonon mode with index k, λ_k is an electron-phonon interaction matrix element, and a_k are bosonic operators for the phonon modes. A key quantity in this model is the phonon spectral density $J(\nu) = \sum_k |\lambda_k|^2 \delta(\nu - \omega_k)$, which we approximate by the contribution from the lowest energy longitudinally polarized mode of the nanowire and a background term arising from other phonon modes in the system [25]

$$J(\nu) = \frac{J_0 d}{c_n \nu}\sin^2(\nu d/c_n)e^{-\nu^2/2\omega_0^2} + J_b(\nu), \quad (2)$$

$$J_b(\nu) = r J_0 \frac{\nu c_n}{d}[1 - \text{sinc}(\nu d/c_n)]e^{-\nu^2/2\omega_0^2}, \quad (3)$$

where J_0 is a constant scale factor, c_n is the phonon speed of sound, d is the spacing between the dots, ω_0 is a cutoff frequency that scales with the size of each dot, and r scales the relative contribution from the background. Numerical values of the fit parameters are listed in the caption of Fig. 2. From this idealized model, we see that the spectral density exhibits oscillations with the phonon energy $\hbar\nu$ when the DQD spacing d is an integer multiple of the phonon wavelength $2\pi c_n/\nu$. This condition allows a simultaneous vibrational antinode at the position of each DQD [10]. Including the tunneling to the left (right) lead at rate $\Gamma_{L(R)}$ in the presence of a source-drain bias, we can derive analytic expressions for the current through the dot (for details of the derivation, see Refs. [10,26]). As seen in the theory curve in Fig. 2(c), modulations in the phonon spectral density show up directly in the current because the charge relaxation rate of the DQD two-level system is directly proportional to $J[\Omega(\epsilon)/\hbar]$.

Going beyond previous experiments, we now report the observation of oscillations in the amplitude and phase response of the cavity that have the same 60 μeV periodicity as the oscillations observed in the current. The cavity transmission, A/A_0, and phase response, $\Delta\phi$, are investigated in Fig. 3 for the lower finite bias triangle of the same interdot transition shown in Fig. 2. These measurements are performed by driving the cavity with an input tone at $f_c = 7782.8$ MHz resulting in an intra-cavity photon number $n_c \approx 50$. The phase response of the cavity [Fig. 3(a)] exhibits oscillations that are once again periodic as a function of detuning (inset), and present throughout the finite bias triangle, suggesting they are caused by an energy-dependent decay mechanism. These features are more clearly visible in $\partial^2\Delta\phi/(\partial V_L \partial V_R)$ [Fig. 3(b)]. Figure 3(c) shows A/A_0 and $\Delta\phi$ as a function of detuning ϵ, measured along the same
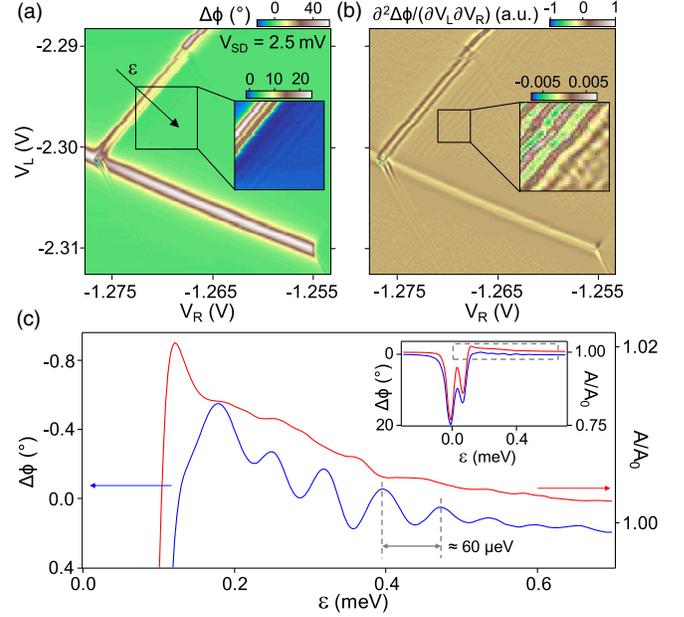

FIG. 3. (a) Cavity phase response $\Delta\phi$ as a function of V_L and V_R near the lower finite bias triangle. (b) Second derivative $\partial^2\Delta\phi/(\partial V_L \partial V_R)$ of the data in (a). (c) $\Delta\phi$ and A/A_0 as a function of detuning ϵ. Inset: Full range of data. The subset of data shown in the main panel is outlined by the dashed grey box. A/A_0 is normalized to the value in Coulomb blockade.

detuning axis as in Fig. 2(c). At positive detuning, clear oscillations are visible in $\Delta\phi$ with a period of approximately 60 μeV. Data are shown over a larger range of detuning in the inset. The dip in transmission and large phase shift near $\epsilon = 0$ are due to the dispersive interaction of the DQD and cavity photons [23]. The second dip in transmission around $\epsilon \approx 70$ μeV may be due to a low lying excited state, although the energy scale is more consistent with the periodic oscillations observed in I, A/A_0, and $\Delta\phi$. The features that we observe at large detuning in A/A_0 and $\Delta\phi$ are also independent of small perturbations in the barrier gate voltage, V_M, suggesting they are a robust consequence of coupling to the phonon bath.

It is helpful to search for correlations between the oscillations observed in the current and the oscillations observed in the cavity response. In general, the energy emitted into the environment during inelastic interdot tunneling is given by the DQD energy splitting $\Omega(\epsilon)$. Energy can be released into the environment by creating phonons and cavity photons. Previous experiments show that roughly one photon is emitted into the cavity mode for every 10^3–10^4 electron tunneling events [33]. Therefore the electronic current primarily probes the phonon environment and should scale as $I(\epsilon)/|e| \propto J[\Omega(\epsilon)/\hbar]$. In contrast, second order processes, where a cavity photon and phonon are emitted during inelastic tunneling, scale with the phonon spectral density $J(\nu)$ as $J[\Omega(\epsilon)/\hbar - 2\pi f_c]$. These processes are illustrated in the inset of Fig. 4(a). For the
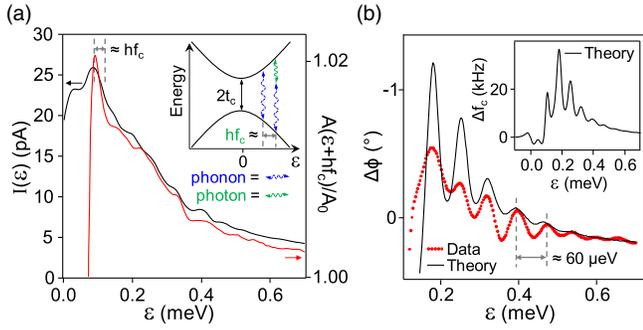
FIG. 4. (a) A comparison of $I(\epsilon)$ and $A(\epsilon + hf_c)/A_0$. Inset: DQD energy level diagram showing the first order emission of a phonon (blue) or the second order emission of the same phonon and a photon (green) of energy hf_c, which occurs when ϵ increases by approximately hf_c. (b) $\Delta\phi$ as a function of ϵ (red) and theory fit (black). The theory curve takes into account the dispersive cavity shift (inset) that is caused by the coupling of cavity photons to nanowire phonon modes. These data, and the Fig. 2(c) data, are simultaneously fit.

large level detunings examined here, $|\epsilon| \gg t_c$, and $\Omega \approx \epsilon$. As such, there should be a correlation between the measured current $I(\epsilon)$ and cavity response $A(\epsilon + hf_c)/A_0$.

Figure 4(a) plots $I(\epsilon)$ and $A(\epsilon + hf_c)/A_0$. The y-axes offsets and data ranges have been adjusted such as to maximize overlap between the two distinct data sets. For $\epsilon > 0.1$ meV there is a strong correlation between $I(\epsilon)$ and $A(\epsilon + hf_c)/A_0$. Both data sets have a very similar inelastic tail. Moreover, the oscillations in $I(\epsilon)$ occur at the same values of detuning as the oscillations in $A(\epsilon + hf_c)/A_0$. These data give further evidence that the oscillations in the current and cavity response are due to the same electron-phonon coupling mechanism.

The cavity phase response can be modeled using a theory that takes into account the dispersive shift of the cavity (renormalization of the cavity frequency) due to the DQD-mediated coupling to nanowire phonons [26]. Measurements of $\Delta\phi$ and best fits to the microscopic theory are shown in Fig. 4(b). The theoretical predictions for the dispersive cavity shift due to electron-phonon coupling are shown in the inset of Fig. 4(b). In comparison with previous theoretical analysis of these systems [25,35], our theory accounts for small energy shifts in the cavity frequency that arise from resonant coupling of the cavity photons to the nanowire phonons when the DQD is in the excited state [26]. The periodic oscillations in the phase arise because periodic modulations in the charge relaxation rate lead to a similar modulation in the excited state population, which shifts the cavity frequency, as seen in the inset of Fig. 4(b). The microscopic origin of the oscillations in our model is identical across all three independent measurement techniques of dc current I, cavity amplitude A/A_0, and phase $\Delta\phi$ [see Eq. (2)], which provides strong evidence that we have observed direct signatures of the electron-phonon coupling in this system.

Future work on suspended nanowires could explore the dependence of the phonon periodicity on the source-drain electrode spacing. Such experiments could help to resolve the conflicting interpretations of the cause of this periodicity in Refs. [13,14]. More broadly, the principles of phonon spectrum engineering and measurement suggested by this work may help to minimize electron-phonon interaction processes at specific energies. For example, single spin relaxation times in III/V semiconductor quantum dots [36,37] are due to spin-orbit coupling and phonon emission [5,7,38]. By tailoring the phonon spectrum, it may be feasible to extend electron spin lifetimes in quantum devices [39].

In summary, we have shown that it is possible to create a cavity-coupled InAs nanowire DQD that is mechanically suspended above the substrate. Consistent with earlier work, we observe oscillations in the inelastic current as a function of level detuning due to electron-phonon coupling in the nanowire [13,14]. Measurements of the cavity response are also sensitive to electron-phonon coupling. We couple the electronic dipole moment of an electron trapped in this DQD to the electric field of a microwave cavity and observe a periodic cavity phase response due to a dispersive interaction with nanowire phonons. A comparison of these measurements with a microscopic theoretical model of the device suggests that the coupling of phonons to photons, mediated by electron dynamics, results in a phonon renormalization of the cavity center frequency. These experiments broadly help to understand the fundamental nature of electron-phonon coupling in nanoscale systems and may provide a path toward mitigating spin decay in semiconductor quantum devices.

[1] M. Dresselhaus, G. Dresselhaus, R. Saito, and A. Jorio, Raman spectroscopy of carbon nanotubes, Phys. Rep. 409, 47 (2005).

[2] Z. Yao, C. L. Kane, and C. Dekker, High-Field Electrical Transport in Single-Wall Carbon Nanotubes, Phys. Rev. Lett. 84, 2941 (2000).

[3] A. Javey, J. Guo, Q. Wang, M. Lundstrom, and H. Dai, Ballistic carbon nanotube field-effect transistors, Nature (London) 424, 654 (2003).

[4] J.-Y. Park, S. Rosenblatt, Y. Yaish, V. Sazonova, H. stnel, S. Braig, T. A. Arias, P. W. Brouwer, and P. L. McEuen, Electron-phonon scattering in metallic single-walled carbon nanotubes, Nano Lett. 4, 517 (2004).

[5] A. V. Khaetskii and Y. V. Nazarov, Spin-flip transitions between Zeeman sublevels in semiconductor quantum dots, Phys. Rev. B 64, 125316 (2001).

[6] W. G. van der Wiel, S. De Franceschi, J. M. Elzerman, T. Fujisawa, S. Tarucha, and L. P. Kouwenhoven, Electron transport through double quantum dots, Rev. Mod. Phys. 75, 1 (2002).

[7] R. Hanson, L. P. Kouwenhoven, J. R. Petta, S. Tarucha, and L. M. K. Vandersypen, Spins in few-electron quantum dots, Rev. Mod. Phys. 79, 1217 (2007).

[8] I. Wilson-Rae, P. Zoller, and A. Imamoḡlu, Laser Cooling of a Nanomechanical Resonator Mode to Its Quantum Ground State, Phys. Rev. Lett. 92, 075507 (2004).

[9] S. Zippilli, G. Morigi, and A. Bachtold, Cooling Carbon Nanotubes to the Phononic Ground State with a Constant Electron Current, Phys. Rev. Lett. 102, 096804 (2009).

[10] T. Brandes and B. Kramer, Spontaneous Emission of Phonons by Coupled Quantum Dots, Phys. Rev. Lett. 83, 3021 (1999).

[11] T. Brandes, Coherent and collective quantum optical effects in mesoscopic systems, Phys. Rep. 408, 315 (2005).

[12] C. Weber, G. Lindwall, and A. Wacker, Zero-phonon line broadening and satellite peaks in nanowire quantum dots: The role of piezoelectric coupling, Phys. Status Solidi B 246, 337 (2009).

[13] C. Weber, A. Fuhrer, C. Fasth, G. Lindwall, L. Samuelson, and A. Wacker, Probing Confined Phonon Modes by Transport through a Nanowire Double Quantum Dot, Phys. Rev. Lett. 104, 036801 (2010).

[14] P. Roulleau, S. Baer, T. Choi, F. Molitor, J. Guttinger, T. Müller, S. Droscher, K. Ensslin, and T. Ihn, Coherent electron-phonon coupling in tailored quantum systems, Nat. Commun. 2, 239 (2011).

[15] T. Fujisawa, T. H. Oosterkamp, W. G. van der Wiel, B. W. Broer, R. Aguado, S. Tarucha, and L. P. Kouwenhoven, Spontaneous Emission Spectrum in Double Quantum Dot Devices, Science 282, 932 (1998).

[16] K. Flohr et al., Manipulating InAs nanowires with submicrometer precision, Rev. Sci. Instrum. 82, 113705 (2011).

[17] H. A. Nilsson, T. Duty, S. Abay, C. Wilson, J. B. Wagner, C. Thelander, P. Delsing, and L. Samuelson, A radio frequency single-electron transistor based on an InAs/InP heterostructure nanowire, Nano Lett. 8, 872 (2008).

[18] M. Aspelmeyer, T. J. Kippenberg, and F. Marquardt, Cavity optomechanics, Rev. Mod. Phys. 86, 1391 (2014).

[19] E. A. Laird, F. Pei, W. Tang, G. A. Steele, and L. P. Kouwenhoven, A high quality factor carbon nanotube mechanical resonator at 39 GHz, Nano Lett. 12, 193 (2012).

[20] N. Ares, T. Pei, A. Mavalankar, M. Mergenthaler, J. H. Warner, G. A. D. Briggs, and E. A. Laird, Resonant Optomechanics with a Vibrating Carbon Nanotube and a Radio-Frequency Cavity, Phys. Rev. Lett. 117, 170801 (2016).

[21] T. Frey, P. J. Leek, M. Beck, A. Blais, T. Ihn, K. Ensslin, and A. Wallraff, Dipole Coupling of a Double Quantum Dot to a Microwave Resonator, Phys. Rev. Lett. 108, 046807 (2012).

[22] M. R. Delbecq, V. Schmitt, F. D. Parmentier, N. Roch, J. J. Viennot, G. Fève, B. Huard, C. Mora, A. Cottet, and T. Kontos, Coupling a Quantum Dot, Fermionic Leads, and a Microwave Cavity on a Chip, Phys. Rev. Lett. 107, 256804 (2011).

[23] K. D. Petersson, L. W. McFaul, M. D. Schroer, M. Jung, J. M. Taylor, A. A. Houck, and J. R. Petta, Circuit quantum electrodynamics with a spin qubit, Nature (London) 490, 380 (2012).

[24] Y.-Y. Liu, J. Stehlik, C. Eichler, M. J. Gullans, J. M. Taylor, and J. R. Petta, Semiconductor double quantum dot micromaser, Science 347, 285 (2015).

[25] M. J. Gullans, Y.-Y. Liu, J. Stehlik, J. R. Petta, and J. M. Taylor, Phonon-Assisted Gain in a Semiconductor Double Quantum Dot Maser, Phys. Rev. Lett. 114, 196802 (2015).

[26] M. J. Gullans, J. M. Taylor, and J. R. Petta, Probing electron-phonon interactions in the charge-photon dynamics of cavity-coupled double quantum dots, Phys. Rev. B 97, 035305 (2018).

[27] M. D. Schroer and J. R. Petta, Correlating the nanostructure and electronic properties of InAs nanowires, Nano Lett. 10, 1618 (2010).

[28] M. D. Schroer, S. Y. Xu, A. M. Bergman, and J. R. Petta, Development and operation of research-scale III–V nanowire growth reactors, Rev. Sci. Instrum. 81, 023903 (2010).

[29] S. Nadj-Perge, S. M. Frolov, E. P. A. M. Bakkers, and L. P. Kouwenhoven, Spin-orbit qubit in a semiconductor nanowire, Nature (London) 468, 1084 (2010).

[30] Y.-Y. Liu, J. Stehlik, C. Eichler, X. Mi, T. R. Hartke, M. J. Gullans, J. M. Taylor, and J. R. Petta, Threshold Dynamics of a Semiconductor Single Atom Maser, Phys. Rev. Lett. 119, 097702 (2017).

[31] J. Stehlik, Y.-Y. Liu, C. M. Quintana, C. Eichler, T. R. Hartke, and J. R. Petta, Fast Charge Sensing of a Cavity-Coupled Double Quantum Dot Using a Josephson Parametric Amplifier, Phys. Rev. Applied 4, 014018 (2015).

[32] See Supplemental Material at http://link.aps.org/supplemental/10.1103/PhysRevLett.120.097701 for additional data and an estimate of the nanowire phonon energy scale.

[33] Y.-Y. Liu, K. D. Petersson, J. Stehlik, J. M. Taylor, and J. R. Petta, Photon Emission from a Cavity-Coupled Double Quantum Dot, Phys. Rev. Lett. 113, 036801 (2014).

[34] A. Stockklauser, V. F. Maisi, J. Basset, K. Cujia, C. Reichl, W. Wegscheider, T. Ihn, A. Wallraff, and K. Ensslin, Microwave Emission from Hybridized States in a Semiconductor Charge Qubit, Phys. Rev. Lett. 115, 046802 (2015).

[35] C. Müller and T. M. Stace, Deriving Lindblad master equations with Keldysh diagrams: Correlated gain and loss in higher order perturbation theory, Phys. Rev. A 95, 013847 (2017).

[36] J. M. Elzerman, R. Hanson, L. H. Willems van Beveren, B. Witkamp, L. M. K. Vandersypen, and L. P. Kouwenhoven, Single-shot read-out of an individual electron spin in a quantum dot, Nature (London) 430, 431 (2004).

[37] T. Meunier, I. T. Vink, L. H. W. van Beveren, K.-J. Tielrooij, R. Hanson, F. H. L. Koppens, H. P. Tranitz, W. Wegscheider, L. P. Kouwenhoven, and L. M. K. Vandersypen, Experimental Signature of Phonon-Mediated Spin Relaxation in a Two-Electron Quantum Dot, Phys. Rev. Lett. 98, 126601 (2007).

[38] A. V. Khaetskii and Y. V. Nazarov, Spin relaxation in semiconductor quantum dots, Phys. Rev. B 61, 12639 (2000).

[39] M. Trif, V. N. Golovach, and D. Loss, Spin dynamics in InAs nanowire quantum dots coupled to a transmission line, Phys. Rev. B 77, 045434 (2008).